

# Structural Studies of the Qarakhanid Dirham Using X-Ray Diffraction and Neutron Tomography Methods

B. A. Abdurakhimov<sup>a, b, \*</sup>, M. Yu. Tashmetov<sup>a</sup>, B. A. Bakirov<sup>b, c, \*\*</sup>, B. S. Yuldashev<sup>a</sup>, S. E. Kichanov<sup>b, \*\*\*</sup>,  
D. P. Kozlenko<sup>b</sup>, and N. B. Ismatov<sup>a</sup>

<sup>a</sup> Institute of Nuclear Physics, Academy of Sciences of the Republic of Uzbekistan, Tashkent, 100214 Republic of Uzbekistan

<sup>b</sup> FLNP, Joint Institute for Nuclear Research, Dubna, 141980 Russia

<sup>c</sup> Kazan (Volga Region) Federal University, Kazan, Republic of Tatarstan, 420008 Russia

\*e-mail: bekhzod@jinr.ru

\*\*e-mail: bulatbakirov4795@gmail.com

\*\*\*e-mail: ekich@nf.jinr.ru

Received April 23, 2021; revised May 24, 2021; accepted May 30, 2021

**Abstract**—The structure and spatial distribution of corrosion in the volume of the medieval Qarakhanid dirham dated the X–XII century A.D. (Anno Domini) has been investigated using non-destructive structural X-ray diffraction and neutron tomography methods. The phase composition and their spatial distribution inside the coins were obtained. The main phase of the studied dirham is the silver-copper alloy with copper fraction dominance up to 74 wt %. The basic phases of the corrosion fraction are cuprite  $\text{Cu}_2\text{O}$ , tenorite  $\text{CuO}$  and chalcocite  $\text{Cu}_2\text{S}$ . The non-uniform distribution of the corrosion penetration in the coin bulk was constructed.

**Keywords:** Qarakhanid dirhams, silver-copper coins, corrosion penetration, non-destructive structural testing, X-ray diffraction, neutron tomography

**DOI:** 10.1134/S1027451021060021

## INTRODUCTION

Recently, a significant interest in the non-destructive structural study of cultural heritage objects in the world archaeological and historical scientific communities increases [1–3]. This is due to the non-destructive careful essence of those experimental studies, in which cultural heritage items with a significant museum or historical value retain their original state after the completion of the research and provide valuable comprehensive scientific data. On the basis of these natural science results, it is possible to suppose new or advanced concepts or ideas for the development of a certain historical nation or cultural groups, the technology and manufacturing growth, and trade relations and influences. From this point of view, the numismatic objects can serve as indicators of historical economic processes, as well as the stages of development of coinage technology [4–8]. The coins are quite often found in most archaeological works or in the discovery of ancient treasures [4, 9].

Like other metal ancient objects of cultural heritage, the coins have a problem of preservation and partial or complete destruction due to corrosion processes over time [7, 10–13]. The main reason is interaction with a chemically aggressive environment like the

atmosphere, salted water, alkaline soil [8, 13–15]. Additional, failure to the conditions of careful storage and improper preservation takes place also. Therefore, there are quite a lot of experimental and theoretical works on research and explanations of corrosion processes [13, 14] and ways of their penetration into copper, silver or gold coins [16, 17]. We believe that modern methods of structural non-destructive diagnostics [18] of the corroded coins can provide relevant data for the required basis of such research. And in particular, typical archaeometry methods like X-ray fluorescence, optical and electron microscopy have significant limitations at the depth of penetration [19–21]. The natural experimental methods with deep penetration into the bulk of the coins [22, 23] look quite promising. The modern X-ray diffraction is a common structural method for the phase analysis of materials and well established as the identification of the phases of numismatic items [6–8, 10, 12]. Another, a little-known structural method is neutron radiography and tomography, which provides an opportunity to obtain an arrangement of the hidden internal components [18, 23–25], the spatial distribution of chemical phases in the volume of massive metal objects. The high penetration depth of neutrons is crucial for the



Fig. 1. The photo of the obverse and reverse side of the studied dirham of Qarakhanid Khanate.

study of metal coins with strong corrosion penetration into the volume.

A corroded copper-silver coin belonging to the Qarakhanid (Persian: قراخانیان) dynasty between the 10th and 13th centuries A.D. (Anno Domini) was chosen as a model object of the cultural heritage of modern Uzbekistan. The area of Qarakhanid side by side with the famous Samanid Emirate, and even successfully fought with them [26, 27]. It should be noted that the chronology of the reign of the Qarakhanid Khans and Ilaks, the dates and places of issue, the names and titles of the Khans, clarifying the complex dynastic relationships between the Kham and Ilaks are also established by coins [26]. We investigated a rather rare copper-silver dirham, which is an archeologic marker of the historical period of the “silver crisis” [28, 29], which led to a sharp drop in the silver content of coins. In this case, we should expect the development of quite complex processes [21] of the corrosion propagation.

In order to expand our knowledge of coins of the Qarakhanid Khanate and, in particular, the coin preservation condition or corrosion spatial propagations into its bulk, we had performed experiments on non-destructive structural diagnostics of the copper-silver coin using X-ray diffraction and neutron tomography method.

## EXPERIMENTAL

The photo of the studied dirham of the Qarakhanid Khanate is shown in Fig. 1. The coin obverse has a traditional pattern kalima in the center. A circular inscription along the edge is not preserved. The corroded reverse side indicates characteristic features of the inscription with indicating the region of coinage – Shash [30–32]. The coin has an irregular rounded

shape, the diameter is about 28 mm, the weight is ~2.9 g. The dark and brown areas of patina or corrosion are visible on both sides.

The phase analyses of coin and corrosion materials were studied using the X-ray diffraction (XRD) method with an EMPYREAN PAN analytical diffractometer (Malvern, Worcestershire, UK). The common  $\text{CuK}\alpha$  radiation with wavelength  $\lambda = 1.54 \text{ \AA}$  was used. The XRD patterns were recorded in the scattering angle range  $20^\circ$ – $120^\circ$  with a scan rate of  $0.33 \text{ deg/min}$ . The diffraction pattern was analyzed by the Rietveld method [33] using the Fullprof software package [34, 35].

The neutron tomography experiments were performed at the neutron radiography and tomography facility [36] placed on the 5<sup>th</sup> beamline of the WWR-SM research reactor (Tashkent, Uzbekistan). A set of neutron radiography images has been collected by the detector system based on the ProLine PL-09000 CCD camera with a maximum field of view of  $90 \times 90 \text{ mm}$ . The tomography experiments were performed using the circular goniometer with a rotation step of  $0.45^\circ$ . The total number of measured radiography projections was 400. The exposure time for one projection was 3 s, and the resulting measurements lasted for 34 min. The imaging data were corrected by the camera dark current image and normalized to the image of the incident neutron beam using the ImageJ software [37]. The tomographic reconstruction was performed by the SYRMEP Tomo Project (STP) software [38]. Finally, a large data set containing a volume distribution of 3D pixels (voxels) were collected. The size of one voxel in our studies is  $61 \times 61 \times 61 \text{ }\mu\text{m}$ . The 3D volume data of voxels are the essence of the spatial distribution of values of the neutron attenuation coefficients inside the sample volume. Attenuation of the neutron beam corresponds to scattering and absorp-

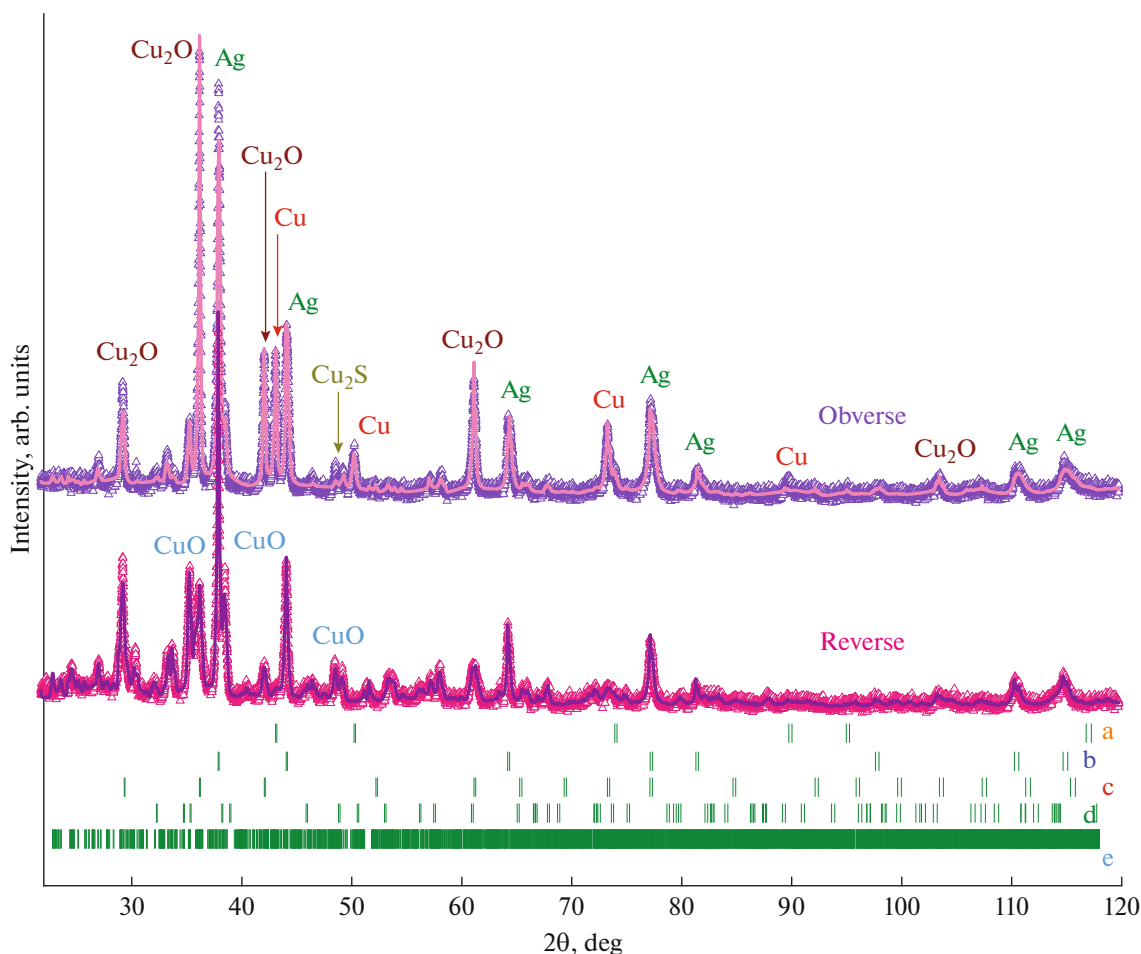


**Fig. 2.** X-ray diffraction patterns of the obverse and reverse sides of the dirham. The experimental points and the calculated profile obtained by the Rietveld method are shown. Ticks below represent calculated positions of the Bragg peaks of the observed phases: (a) silver, (b) copper, (c) cuprite, (d) tenorite, (e) chalcocite. The several characteristic diffraction peaks of different phases are marked.

tion losses inside the material [24, 39] depending on the elementary composition of an investigated object. The 3D viewer plugin [40] of the ImageJ is used for visualization and simple analysis of reconstructed 3D data.

## RESULTS AND DISCUSSION

### *X-ray Diffraction*

The X-ray diffraction patterns obtained for both obverse and reverse sides of the studied dirham are shown in Fig. 2. The well-separated diffraction peaks of copper and silver phases are observed. The analysis of diffraction patterns using the Rietveld method provides the average content of the copper and silver phases as  $25.5 \pm 1.0\%$  and  $74.5 \pm 1.0\%$ . This corresponds to the mass ratios as 17:83. There are quite a few diffraction peaks that relate to corrosion on the surface of the dirham. Diffraction data analysis indicates the several phases that content the corroded

material: cuprite  $\text{Cu}_2\text{O}$ , tenorite  $\text{CuO}$ , and chalcocite  $\text{Cu}_2\text{S}$ . It is assumed, the cuprite phase is associated with brown-color areas of the patina, while the tenorite and chalcocite phases are related to dark regions of surface corrosion. The lattice parameters of observed phases of the studied dirham are listed in Table 1.

The mineral composition of the patina indicates a long stay of the dirham in a saline environment, presumably in soil or sand. The absence of mineral chlorine markers such as chlorargyrite or atacamite can indicate indirectly a lack of prolonged contact with the atmosphere.

It can be seen that the intensity of the diffraction peaks for different phases depends quite strongly on the local effects like the obverse and reverse sides of the dirham. This may be due to the strong unevenness of the spatial distribution of both the main copper and silver phases and the minor phases of corrosion. For a more detailed study of the spatial distribution of the

**Table 1.** The space group and lattice parameters of observed phases of the studied dirhem

Phase	Space group	Lattice parameters
Silver	$Fm\bar{3}m$	$a = 4.086(3) \text{ \AA}$
Copper	$Fm\bar{3}m$	$a = 3.615(2) \text{ \AA}$
Cuprite	$Pm\bar{3}m$	$a = 4.273(2) \text{ \AA}$
Tenorite	$C2/c$	$a = 4.684(3) \text{ \AA}, b = 3.423(5) \text{ \AA}, c = 5.123(3) \text{ \AA}, \beta = 99.5(5)^\circ$
Chalcocite	$P2_1/c$	$a = 15.246(6) \text{ \AA}, b = 11.884(8) \text{ \AA}, c = 13.494(6) \text{ \AA}, \beta = 116.4(6)^\circ$

composite phases of the dirham, neutron tomography studies were provided.

### Neutron Tomography

The attenuation coefficient of a neutron beam for silver is almost an order of magnitude greater than the corresponding coefficient for copper [41] and copper oxides. In this case, good radiographic contrast in neutron radiography and tomography experiments is expected. Indeed, on the reconstructed from neutron tomography three-dimensional 3D model of the dirham, it is easy to separate spatial distribution of different phases (Fig. 3a). High penetration of corrosion

inside the coin volume is visible. From the neutron tomography data, it is possible to estimate the volumes of the copper-silver material and the volume of the corroded areas. The total volume of the studied dirham is formed by 1558071 voxels or 353 mm<sup>3</sup>. The volume of preserved copper-silver material occupies 218 mm<sup>3</sup> or 61.7% of the total volume of the coin. Interestingly, silver and copper are unevenly distributed in the preserved metal fragment (Fig. 3b) and the volume of the silver-rich part does not exceed 73 mm<sup>3</sup>. Several transversal slices of the reconstructed 3D model of the coin are presented in Fig. 3c. It is visual that in several points corrosion matter completely replaces the metal part of the coin. The thickness of the corrosion layer varies from several tens of microns to the full thickness of the coin of 0.8 mm.

A comparison of the reconstructed 3D model of the coin with the photo (Fig. 1) indicates the cuprite phase as a matter of the maximum penetration of corrosion into the volume of dirham. The remaining phases of corrosion are associated rather with the surface location. In accordance with the data of the work [16], the corrosive material is localized in the areas with the dominant copper content of the copper-silver coins. We assumed, that the degradation [21] of the copper content of the coin leads to the redistribution of the dominant phase of the observed Cu-Ag alloy towards silver content. Therefore, the X-ray diffraction data indicate an increased silver content of up to 74.5%. If we take into account the volume of the dirham, the total silver content in the studied coin reaches 26 wt % or 0.76 g. It should note, the areas with dominant silver content are observed in the volume of the ancient copper-silver coins [16, 21, 23].

### CONCLUSION

The heavily corroded dirham of the Qarakhanid Khanate has been studied using non-destructive structural diagnostics like X-ray diffraction and neutron tomography methods. The main phase of the copper-silver coin as well as the corrosion matter was obtained. The cuprite, tenorite, and chalcocite phases of corrosion indicate a long stay of the studied dirham in the soil environment without sufficient air access. The reconstructed neutron tomography data visualize a deep penetration of corrosion, mainly cuprite phase,

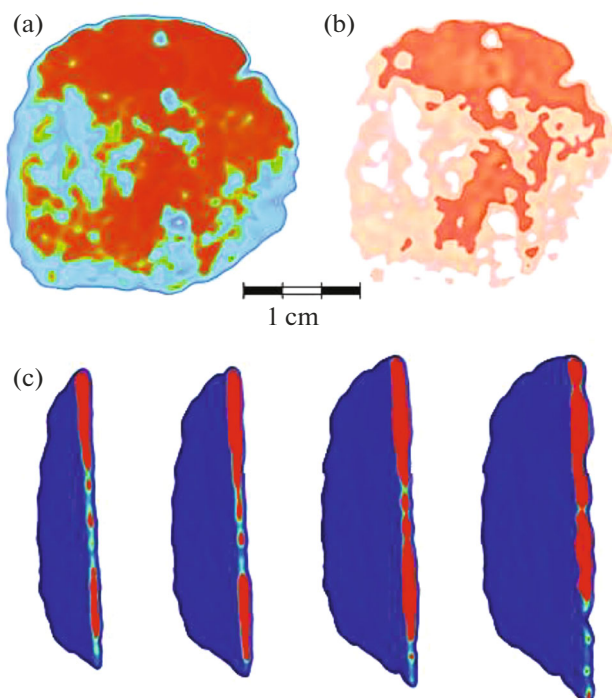


**Fig. 3.** The 3D model of the coin reconstructed from the neutron-tomography data (a) and preserved copper-silver material of the coin (b). Several longitudinal virtual slices of the reconstructed 3D model (c). It is assumed that the red areas correspond to the metal phase, while the blue areas are corrosion products. The rainbow-like coloring shows neutron absorption degree from low (blue) to high (red).

into the volume of the dirham. Due to the strong degradation of the copper component of the studied coin, the dominance of the silver phase in the volume of the studied dirham is founded.

## REFERENCES

1. *Non-Destructive Micro Analysis of Cultural Heritage Materials*, Ed. by K. Janssens and R. Van Grieken (Elsevier, Amsterdam, 2005).
2. A. Adriaens, *Spectrochim. Acta, Part B* **60**, 1503. (2005). <https://doi.org/10.1016/j.sab.2005.10.006>
3. E. H. Lehmann, P. Vontobel, E. Deschler-Erb, and M. Soares, *Nucl. Instrum. Methods Phys. Res., Sect. A* **542**, 68 (2005). <https://doi.org/10.1016/j.nima.2005.01.013>
4. F. Kemmers and N. Myrberg, *Archaeol. Dialogues* **18**, 87 (2011). <https://doi.org/10.1017/S1380203811000146>
5. S. Davis, *Acta Classica: Proc. Classical Assoc. S. Afr.* **3**, 67 (1960). [https://doi.org/10.10520/AJA00651141\\_54](https://doi.org/10.10520/AJA00651141_54)
6. M. di Fazio, F. di Turo, L. Medeghini, L. Fabrizi, F. Catalli, and C. de Vito, *Microchem. J.* **144**, 309 (2019). <https://doi.org/10.1016/j.microc.2018.09.016>
7. L. Fabrizi, F. di Turo, L. Medeghini, M. di Fazio, F. Catalli, and C. de Vito, *Microchem. J.* **145**, 419 (2019). <https://doi.org/10.1016/j.microc.2018.10.056>
8. A. Mezzi, C. Riccucci, T. de Caro, E. Angelini, F. Faraldi, S. Grassini, and V. K. Gouda, *Surf. Interface Anal.* **10–11**, 801 (2014). <https://doi.org/10.1002/sia.5385>
9. K. Lockyear, *Oxford J. Archaeol.* **31**, 191 (2012). <https://doi.org/10.1111/j.1468-0092.2012.00385.x>
10. C. M. B. Martins and J. I. Martins, *Prot. Met. Phys. Chem. Surf.* **47**, 128 (2011). <https://doi.org/10.1134/S2070205110061012>
11. A. Kirfel, W. Kockelmann, and P. Yule, *Archaeometry* **53**, 930 (2011). <https://doi.org/10.1111/j.1475-4754.2011.00588.x>
12. R. C. Fierascu, I. Fierascu, A. Ortan, F. Constantin, D. A. Mirea, and M. Statescu, *Nucl. Instrum. Methods Phys. Res., Sect. B* **401**, 18 (2017). <https://doi.org/10.1016/j.nimb.2017.04.030>
13. A. Doménech, M. T. Doménech-Carbó, T. Pasies, and M. del Carmen Bouzas, *Electroanalysis* **24**, 1945 (2012). <https://doi.org/10.1002/elan.201200252>
14. M. P. Casaletto, G. M. Ingo, C. Riccucci, and F. Faraldi, *Appl. Phys. A: Mater. Sci. Proces.* **100**, 937 (2010). <https://doi.org/10.1007/s00339-010-5677-1>
15. D. W. Rice, P. Peterson, E. B. Rigby, P. B. P. Phipps, and R. J. Cappell, *J. Electrochem. Soc.* **128**, 275 (1981). <https://doi.org/10.1149/1.2127403>
16. F. Salvemini, S. R. Olsen, V. Luzin, U. Garbe, J. Davis, T. Knowles, and K. Sheedy, *Mater. Charact.* **118**, 175 (2016). <https://doi.org/10.1016/j.matchar.2016.05.018>
17. S. E. Kichanov, K. Nazarov, D. Kozlenko, I. Saprykina, E. Lukin, and B. Savenko, *J. Surf. Invest.: X-ray, Synchrotron Neutron Tech.* **11**, 585 (2017). <https://doi.org/10.1134/S1027451017030296>
18. *Neutron Applications in Earth, Energy and Environmental Sciences*, Ed. by R. Rinaldi, L. Liang, and H. Schober, *Neutron Scattering Applications and Techniques*, Ed. by I. S. Anderson, A. J. Hurd, and R. L. McGreevy (Springer, New York, 2009); *Neutron Imaging and Applications: A Reference for the Imaging Community*, Ed. by I. S. Anderson, R. L. McGreevy, H. Z. Bilheux, and Z. Hassina, *Neutron Scattering Applications and Techniques*, Ed. by I. S. Anderson, A. J. Hurd, and R. L. McGreevy (Springer, New York, 2009).
19. J. Tate, *Nucl. Instrum. Methods Phys. Res., Sect. B* **14**, 20 (1986). [https://doi.org/10.1016/0168-583X\(86\)90417-9](https://doi.org/10.1016/0168-583X(86)90417-9)
20. G. Weber, J. Guillaume, D. Strivay, H.P. Garnir, A. Marchal, and L. Martinot, *Nucl. Instrum. Methods Phys. Res., Sect. B* **161–163**, 724 (2000). [https://doi.org/10.1016/S0168-583X\(99\)00948-9](https://doi.org/10.1016/S0168-583X(99)00948-9)
21. L. Beck, S. Bosonnet, S. Réveillon, D. Eliot, and F. Pilon, *Nucl. Instrum. Methods Phys. Res., Sect. B* **226**, 153 (2004). <https://doi.org/10.1016/j.nimb.2004.06.044>
22. M. Abramson, I. Saprykina, S. E. Kichanov, D. P. Kozlenko, and K. Nazarov, *J. Surf. Invest.: X-ray, Synchrotron Neutron Tech.* **12**, 114 (2018). <https://doi.org/10.1134/S1027451018010202>
23. B. Bakirov, S. E. Kichanov, R. Khrumchenkova, A. Belushkin, D. Kozlenko, and A. Sitdikov, *J. Surf. Invest.: X-ray, Synchrotron Neutron Tech.* **14**, 376 (2020). <https://doi.org/10.1134/S1027451020020433>
24. E. Lehmann, D. Mannes, A. Kaestner, and C. Grünzweig, *Phys. Procedia* **88**, 5 (2017). <https://doi.org/10.1016/j.phpro.2017.06.055>
25. N. Kardjilov, A. Hilger, I. Manke, M. Strobl, W. Treimer, and J. Banhart, *Nucl. Instrum. Methods Phys. Res., Sect. A* **542**, 16 (2005). <https://doi.org/10.1016/j.nima.2005.01.005>
26. M. Biran, “Karakhanid Khanate,” in *The Encyclopedia of Empire*, Ed. by J. M. MacKenzie (Wiley, New York, 2016). <https://doi.org/10.1002/9781118455074.wbeoe156>
27. R. Abazov, “The Karakhanid State (999–1140),” in *The Palgrave Concise Historical Atlas of Central Asia* (Palgrave Macmillan, New York, 2008), pp. 40–41. [https://doi.org/10.1057/9780230610903\\_18](https://doi.org/10.1057/9780230610903_18)
28. T.S. Noonan, *J. Am. Orient. Soc.* **94**, 448 (2011). <https://doi.org/10.2307/600587>
29. R. Naismith, *Numis. Chron.* (1966–) **165**, 193 (2005).
30. B. D. Kochnev, “Set of Inscriptions on Karakhanid Coins: Anthroponyms and Titles (Part 1),” in *Eastern Historical Source Studies and Special Historical Disciplines* (Nauka, Moscow, 1995). [Russian]
31. S. Album, *Checklist of Islamic Coins*, 3rd ed. (Santa Rosa, 2011).
32. M. Fedorov, *Numis. Chron.* (1966–) **160**, 171 (2000).
33. H. M. Rietveld, *J. Appl. Crystallogr.* **2**, 65 (1969). <https://doi.org/10.1107/s0021889869006558>

34. J. Rodríguez-Carvajal, *Phys. B (Amsterdam, Neth.)* **192**, 55 (1993).  
[https://doi.org/10.1016/0921-4526\(93\)90108-I](https://doi.org/10.1016/0921-4526(93)90108-I)
35. J. Rodríguez-Carvajal, “Magnetic Structures from Powder and Single Crystal Data,” in *Applied Crystallography*, Ed. by H. Morawiec and D. Stróz (World Sci., 2014), pp. 30–36.  
[https://doi.org/10.1142/9789812811325\\_0005](https://doi.org/10.1142/9789812811325_0005)
36. B. A. Abdurakhimov, M. Y. Tashmetov, B. S. Yuldashiev, S. E. Kichanov, E. V. Lukin, D. P. Kozlenko, S. A. Kulikov, V. N. Shvetsov, N. B. Ismatov, A. R. Saidov, A. B. Normurodov, and A. V. Rutkauskas, *Nucl. Instrum. Methods Phys. Res., Sect. A* **989** 164959 (2021).  
<https://doi.org/10.1016/j.nima.2020.164959>
37. C. A. Schneider, W. S. Rasband, and K. W. Eliceiri, *Nat. Methods* **9**, 671 (2012).  
<https://doi.org/10.1038/nmeth.2089>
38. F. Brun, L. Massimi, M. Fratini, D. Dreossi, F. Billé, A. Accardo, R. Pugliese, and A. Cedola, *Adv. Struct. Chem. Imaging* **3**, 4 (2017).  
<https://doi.org/10.1186/s40679-016-0036-8>
39. J. J. Rant, Z. Miličič, P. Turk, and I. Lengar, “Neutron Radiography as a NDT Method in Archaeology,” in *Proceedings of the 8th Int. Conf. of the Slovenian Society for Non-Destructive Testing: Application of Contemporary Non-Destructive Testing in Engineering*, Portorož, Slovenia (2005), pp. 181–188.
40. B. Schmid, J. Schindelin, A. Cardona, M. Longair, and M. Heisenberg, *BMC Bioinf.* **11**, 274 (2010).  
<https://doi.org/10.1186/1471-2105-11-274>
41. P. Kienzle, NIST Neutron Activation and Scattering Calculator, NIST Cent. Neutron Res. (2014).